Proceedings of the 2011 IEEE
International Conference on Robotics and Biomimetics
December 7-11, 2011, Phuket, Thailand

Trajectory Planning and Posture Adjustment of a Quadruped Robot for Obstacle Striding

Xuesong Shao, Yiping Yang, Ying Zhang, and Wei Wang

***Abstract*—This paper proposes a control method of trajectory planning and posture adjustment for quadruped robots' obstacle striding. The addressed mixed parabola method plans the travelling paths over obstacles in Cartesian coordinate system. The constraints on velocities, accelerations, and jerks at waypoints are employed to generate the time-efficient smooth cubic spline joint trajectories by nonlinear optimization technique. The planned trajectories maximize the compliance and flexibility of joint movements. To guarantee the static stability for the pitch-pitch type quadruped robots, a posture adjustment strategy based on the potential energy is investigated to regulate the trajectory of Center of Gravity (COG). The experimental results on quadruped robot FROG-I (Four-legged Robot for Optimal Gaits) prove the feasibility of the proposed approach of striding a board in natural environment.**

I. Introduction

MANY investigations of quadruped robots have been done in walking on discontinuous terrain during the past decades. Different experiments proved that compliant locomotion in outdoor environment is more challenging. A great many quadruped robots have been employed in discontinuous terrain experiments, such as Tekken robots [1], [2], SCOUT II [3], SILO4&6 [4], [5], and the LittleDog [6], [7] and BigDog designed by Boston Dynamic Incorporation and so on. Some methods based on Center Pattern Generator (CPG) made up of nonlinear coupling oscillators in terms of neurobiology seem simple in quadruped control, however, the parameters of CPG, without concerning the quadruped kinematics and dynamics, are strongly coupled with each other preventing the complex walking maneuvers [1], [2], [8]. Some other robots' control methods based on the dynamics [9], such as the ones used on SCOUT II and LittleDog, are too complicated to be used on general platforms.

The performance of quadruped robots is affected by several factors including the mechanism, the controller, and the path planner. Different from the others, our approach is realized according to the kinematics, trajectory optimization, and potential energy stability without complicated coupled dynamic calculations. In view of the accumulated error of local coordinate systems changed with links' movement, the Rodrigues formulation [10] is more suitable in modeling of the quadruped robots. Through watching the mammals' obstacle striding, we find that the box-shape traversing path [6] is not conformed to the nature movement which is smooth and flexible. However, the mixed parabola-shape path made up of partitioned parabolas and straight lines performs very well in choosing the feasible waypoints towards obstacles on its discontinuous way. Moreover, the limited velocities, accelerations, and jerks at the waypoints are considered in the cubic spline interpolation so that the trajectory is time-efficient and smooth by nonlinear optimization. In addition, several planning methods [5], [11] on Center of Gravity (COG) trajectory adjustment are available to some quadruped robots, e.g. the LittleDog and SILO6. Nevertheless, with regard to the pitch-pitch type quadruped robots, the stability is a difficult problem to deal with. In this case, to generate enough stability margins, the idea of potential energy method to adjust the COG trajectory is particularly useful in posture adjustment.

The rest of this paper is organized as follows. Section II introduces the quadruped platform and builds up the kinematics model. Section III presents the path planning and trajectory optimization method. In Section IV the potential energy stability measure in COG trajectory adjustment is discussed. The experimental results are shown and analyzed in Section V. Finally, Section VI draws the conclusion and describes the future work.

II. The Quadruped Platform And The Kinematics Model

A. The Quadruped Platform

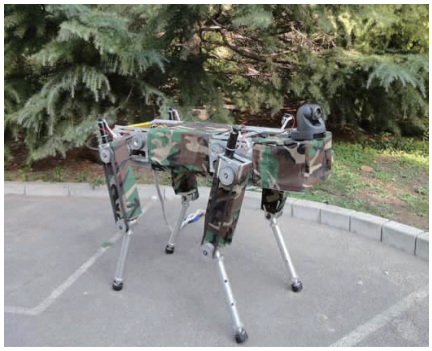

Fig. 1. The FROG-I robot in our lab.

The quadruped robot FROG-I, built in our lab, is about 1150mm long, 700mm wide, and 950mm tall, with a total weight of approximately 55kg. Each leg, known as the

Manuscript received August 10, 2011.

Xuesong Shao, Yiping Yang, and Wei Wang are with the Institute of Automation, Chinese Academy of Sciences, Beijing, China. xuesong.shao@gmail.com, yiping.yang@ia.ac.cn, wei.wang@ia.ac.cn

Ying Zhang is with School of Mechanical Engineering, Beijing Institute of Technology. zhwel329@gmail.com

978-1-4577-2138-0/11/$26.00 © 2011 IEEE

pitch-pitch type leg, contains one hip pitch joint and one knee pitch joint, both of which are powered by DC motors. Still, FROG-I possesses one passive compliant prismatic DOF at each toe which can be used to detect the contact between the foot and the ground. An embedded controller performs sensing and actuator control, and communicates with a Linux host computer through a wireless connection. The gyroscope, camera, foot contact sensors, and joint angle sensors have been installed on the quadruped robot.

B. The Forward Kinematics of the Quadruped Model

Due to the simplicity and flexibility, as well as the accuracy during coordinate transformations, the Rodrigues rotation formula is more applicable in robots' kinematics. The Rodrigues rotation formula which defines the rotation matrix can be expressed as

$$e^{(\mathbf{a}\times 1)\theta} = \mathbf{I} + (\mathbf{a}\times 1)\sin\theta + (\mathbf{a}\times 1)^2(1-\cos\theta), \quad (1)$$

where $\mathbf{I} \in \mathbb{R}^{3\times 3}$ is the identity matrix, θ is the joint angle and $\mathbf{a} \in \mathbb{R}^{3\times 1}$ is the unit vector of the joint velocity $\boldsymbol{\omega}$,which is the joint axis and can be expressed as

$$\boldsymbol{\omega} = \mathbf{a}\omega. \quad (2)$$

Show that

$$\boldsymbol{\omega} = \begin{bmatrix} \omega_x \\ \omega_y \\ \omega_z \end{bmatrix},$$

where ω_x, ω_y, and ω_z describe the components of joint velocity along x, y, and z axes. Next, the description of $\boldsymbol{\omega}\times 1$ is given by

$$\boldsymbol{\omega}\times 1 = \begin{bmatrix} 0 & -\omega_z & \omega_y \\ \omega_z & 0 & -\omega_x \\ -\omega_y & \omega_x & 0 \end{bmatrix}.$$

Based on (2), $\boldsymbol{\omega}\times 1$ can also be written

$$\boldsymbol{\omega}\times 1 = (\mathbf{a}\times 1)\omega. \quad (3)$$

In the same way, the cross product of two vectors could be described in the following form

$$\boldsymbol{\omega}\times\mathbf{p} = (\boldsymbol{\omega}\times 1)\mathbf{p}. \quad (4)$$

According to the above kinematics theories, the orientation and position information of robotic link system can be obtained from two transform equations,

$$\mathbf{p}_j = \mathbf{p}_i + \mathbf{R}_i\mathbf{b}_j, \quad (5)$$

$$\mathbf{R}_j = \mathbf{R}_i e^{(\mathbf{a}_j\times 1)q_j}, \quad (6)$$

where i and j represent the ith link and the jth link respectively, known as the mother link and the child link. $\mathbf{p}$ and $\mathbf{R}$ are the links' position and orientation in the world coordinate system($\sum_W$). $\mathbf{a}$, $\mathbf{b}$, and q are the joint axis vector, relative position vector, and the joint angle with respect to the mother link.

Fig. 2 shows the quadruped kinematics model on the basis of the Rodrigues method. Here, $\mathbf{p}_B$ is the center of the body, RFH, LFH, RHH, and LHH denote the right front hip, left front hip, right hind hip, and left hind hip, respectively. RFK, LFK, RHK, LHK stand for right front knee, left front knee, right hind knee, and left hind knee, and RFF, LFF, RHF, LHF represent right front foot, left front foot, right hind foot, and left hind foot. Taking right front leg as an example, $\mathbf{b}_{RFH}$ is the position of the RFH joint to the center of the body; $\mathbf{b}_{RFK}$ is the position of the RFK joint to the RFH joint; $\mathbf{b}_{RFF}$ is the position of the RFF end effector to the RFK joint; $\mathbf{p}_{RFH}$ and $\mathbf{p}_{RFK}$ are the positions of the RFH joint and the RFK joint to the $\sum_W$; $\mathbf{a}_{RFH}$ and $\mathbf{a}_{RFK}$ are the RFH joint vector and RFK joint vector, which are similar to the other three legs.

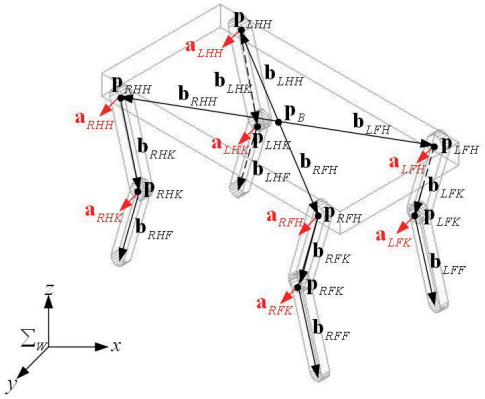

Fig. 2. The quadruped kinematics model.

III. Trajectory Planning

It is known to all that many quadruped robots do not perform well compared with nature quadruped's locomotion especially in respect of the time efficiency and the locomotion smoothness while walking on discontinuous terrain. Therefore, generating feasible trajectory that quadruped robots should follow is significant [12]–[14]. To achieve the goal, path planning should be accomplished firstly to generate the waypoints according to the obstacles' geometrics and robots' kinematics, and then joint trajectories could be obtained from the cubic spline interpolation with the constrained terms and nonlinear optimization technique.

A. Path Planning

Although there are various obstacles difficult to be dealt with in nature environment, the sections of most typical obstacles are approximately round, rectangle or triangle. In order to jump over these obstacles, several strategies can be used to choose the waypoints that the foot should pass through to the goal point. For instance, the box pattern method [6] shown in Fig. 3(a), (b), (c) or the trapezoid pattern method are commonly used due to their simplicity. However, it can be found that there are inflection areas resulting in the motion discontinuous at the four corners in the box-shape path and the safety margins are not considered seriously.

Inspired from biological motion, we investigate the mixed parabola method which selects the waypoints at a path corner

to form a parabola shape and chooses the waypoints along straight lines between the adjacent parabola segments. As shown in Fig. 3(d), (e), (f), three waypoints according to the mixed parabola shape at each corner of quasi-round obstacle, quasi-rectangular obstacle, and quasi-triangular obstacle are reasonably chosen. Some other researchers, for example John R. Rebula [15], considered the parabolic segments at the top of the obstacles with linear segments at lifting up and putting down phrases. However, the path is longer and the waypoints are generated roughly. In addition, to keep safe and improve the efficiency, reasonable safety margins are necessary to be reserved while jumping over obstacles. Finally, we convert the flexible waypoints into joint space, as a series of joint knots, by utilizing the numerical solution [10] of inverse kinematics.

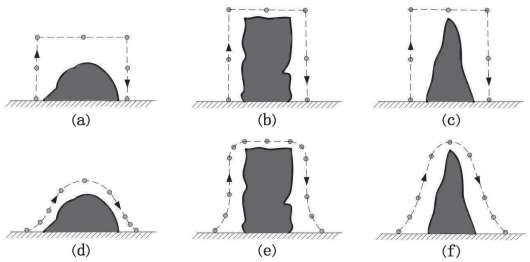

Fig. 3. The waypoints of the paths over obstacles. (a) Box pattern method for quasi-round obstacle. (b) Box pattern method for quasi-rectangular obstacle. (c) Box pattern method for quasi-triangular obstacle. (d) Mixed parabola method for quasi-round obstacle. (e) Mixed parabola method for quasi-rectangular obstacle. (f) Mixed parabola method for quasi-triangular obstacle.

B. Joint Trajectory Optimization

Compared to B-spline which does not pass through the knots of the trajectory precisely, piecewise cubic spline interpolation which can generate simple and twice differentiable trajectory is a popular method used for smooth motion of robots. The constraints on velocities, accelerations, and jerks at the joint knots, as well as the time intervals between the neighboring knots, are crucial elements for fitting parameters of cubic spine with smoothness and efficiency [16]–[18]. If these elements have optimal values, the minimization of the energy consumption, vibration, and mechanical wear can be easily achieved while walking on complicated terrain.

There are many objective functions performing very well in certain conditions in robotics optimization, such as minimizing the total time, maximum velocity, maximum acceleration or average acceleration. In our experiments, taking into account of the time and smoothness items, the sum of the squared accelerations at the waypoints and total time between adjacent waypoints is superior to others. We propose the objective function mathematically as

$$f(\mathbf{h},\mathbf{q}_i^{"}) = m\sum_{j=1}^{n-1} h_j + \sum_{i=1}^{m} tr\mathbf{q}_i^{"T}\mathbf{q}_i^{"}, \tag{7}$$

where i is the ith joint of the m joints corresponding to hip pitch joint and knee pitch joint on one leg; j is the jth position knot on one joint trajectory; $\mathbf{q}_i^{"} = [q_{i1}^{"}, q_{i2}^{"}, \cdots q_{in}^{"}]$ represents the joint acceleration vector over n knots of the ith joint; $\mathbf{h} = [h_1, h_2, \cdots h_{n-1}]$ stands for the time interval vector with $h_j = t_{j+1} - t_j \quad (j = 1,2,\cdots,n-1)$. Also, $t_0 < t_1 < \cdots < t_{n-1} < t_n$ is the time sequence for n knots and q_{ij} is knot value at time t_j of the ith joint.

The mathematical expressions of the constrained items are shown below,

$$\left|q_{ij}^{'}\right| \le v_{i\lim}, \tag{8}$$

$$\left|q_{ij}^{"}\right| \le a_{i\lim}, \tag{9}$$

$$\left|q_{ij}^{"'}\right| \le \sigma_{i\lim}, \tag{10}$$

where $q_{ij}^{'}$, $q_{ij}^{"}$, $q_{ij}^{"'}$ are the velocity, acceleration, and jerk at the jth knot of the ith joint and $v_{i\lim}$, $a_{i\lim}$, $\sigma_{i\lim}$ are the maximum allowable values of the velocity, acceleration, and jerk for the n knots on the ith joint trajectory. Note that, $q_{ij}^{"'} = \dfrac{q_{ij+1}^{"} - q_{ij}^{"}}{h_j}$.

Obviously, the optimization problem mentioned above is nonlinear. As for the constrained nonlinear optimization problems, a great many of mature solutions have been developed, such as constrained complex method, coordinate alternation method, penalty function method [16]. Considering the speed and complexity of the solutions, we solve the problem using the accelerated hybrid penalty function technique.

IV. The Strategy of COG Trajectory Adjustment

Whether the horizontal projection of the COG lies inside the support convex polygon formed by all legs in stance phase decides the stability for static walking [19]. The shortest distance from the COG projection to edges of the polygon defines the stability margin. Larger margins produce a increase in static stability while walking. Furthermore, the COG trajectories' characteristics including deferentiality, sideway amplitudes [20], and backward distances, determine the robots' walking performance to some extent.

Some quadruped robots which have three actuated joints per leg make use of the roll or yaw joint to generate stability margins through swaying the legs sideways to extend the support polygon [5], [11]. For the pitch-pitch type quadruped robots, due to the joint motion limited in the sagittal plane, the robot could not shift the COG sideways to produce more stability margins using roll or yaw joint flexibly. To solve this problem, we propose the strategy of moving the body forwards and backwards while flexing and stretching the diagonal legs simultaneously. Then, the COG projection can be moved to the proper position in the support triangle with adequate margins. With this action, some potential energy is generated to prevent the robots from tumbling down to the direction of the leg in swing phrase. Consequently, we can

evaluate the robots' stability by both the stability margins and the potential energy. Fig. 4 describes the turning of the diagonal legs, and the potential energy ΔE is determined by the drop of COG,

$$\Delta E = mg\Delta h, \tag{11}$$

where m is the mass of the body, g is the acceleration of gravity, and Δh is the vertical drop distance of COG.

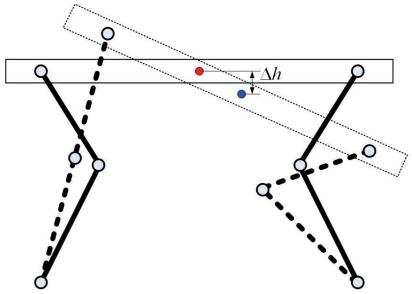

Fig. 4. The turning diagram of diagonal legs.

Fig. 5 illustrates the COG adjustment strategy in a cycle for periodic motion. We divide the period into six states, start state, RF swing state, LH swing state, LF swing state, RH swing state, and recovery state. The start state and the recovery state are in the same posture. The filled circles represent the foot locations and particularly the red circles and the green circles represent the foot locations of the flexed legs and the stretched legs. Also, d defines the stability margins and RF, LF, LH, and RH denote right front, left front, left hind, and right hind as similarly described in Section II. The moving sequence of the four legs is RF-LH-LF-RH.

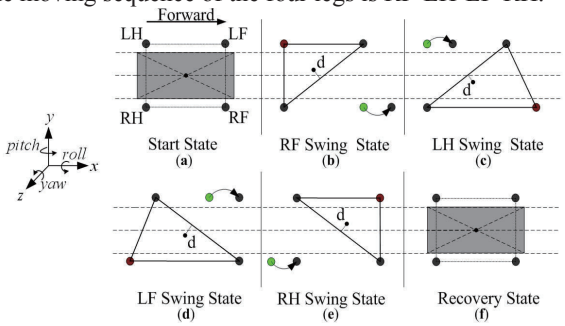

Fig. 5. The adjustment of COG in a cycle for periodic motion.

The explanation of the transitions from one state to the next in Fig. 5 is given in details.

1) Starting from the robot's initial pose shown in Fig. 5(a), the vertical projections of the COG and the geometric center of the body overlap with each other. With flexing the LH leg and stretching the RF leg the body is moved backwards. Therefore, the COG moves to the left-hind direction to generate some margins for the step of RF swing state shown in Fig. 5(b).
2) When RF leg lifts up to move forwards, the LH warped leg extends to normal state and then shifts the body forwards with the other three stance legs. At the time of touching the ground of RF leg, the COG projection arrives at the diagonal line between LF leg and RH leg. For the sake of producing stability margins to perform the LH leg's raising shown in Fig. 5(c), the body should keep on moving forwards with the four stance legs while stretching LH leg and flexing RF leg.
3) At this stage, a noticeable fact is to keep down the distances that the body travels forwards. That is, after LH leg arriving at its desired position, there are certain distances from the COG projection to the diagonal line between RF leg and LH leg. As shown in Fig. 5(d), the purpose is to shorten the distances of moving backwards to obtain enough stability margins with flexing RH leg and stretching LF leg for uplifting LF leg.
4) From the LF swing state to the RH swing state shown in Fig. 5(e), the COG is shifted from right-hind area to left-front area. In the meanwhile, RH leg should be stretched and LF leg should be flexed. There are also two steps like 2), moving the COG projection to the diagonal line of RF leg and LH leg and going on to move the COG projection to left-front support area to generate stability margins for the next step.
5) With the stability margins shown in Fig. 5(e), RH leg travels to the next location. Differently, during this stage, the body is not shifted forwards to prepare for the recovery movement later on. After RH leg arriving at its proper position, all four stance legs move the body backwards and LF leg extends to normal state. Therefore, as result of the sufficient adjustment, the robot comes to the original state.

Actually, the adjusting of the COG trajectory involves several significant factors which are critical to the stability and walking performance:

1) stability margins
2) the extent of stretching or flexing legs
3) stride height and span
4) distances of the forward or backward body movement to keep balance
5) the degree of body roll inclination
6) potential energy for stability

Considering discontinuous terrain, some appropriate measures can be implemented to cope with it. For instance, we can increase the stride span and height, move the body forwards for longer distances, and stretch or flex the legs seriously. Nonetheless, we must draw some attentions between the ability of obstacle striding and the walking performance. It is obvious that the body inclination increases the potential energy for stability but decreases the smoothness of compliant locomotion. Similarly, longer distances of the body travelling during the legs' forward movement generate larger margins, however, it leads to a decrease in continuity because of the pulling back to insure the next step's stability. Acknowledging those points, the obstacles should be passable and reasonable to cross over. Then we can take some of the measures simultaneously to seek a compromise walking maneuver with regards to mammals' behaviors and the robots' locomotion performance.

V. Experiments and Evaluations

We implement the proposed control strategy of striding obstacle on the FROG-I quadruped robot introduced in Section II. The obstacle is a wood board, 1500mm in length, 110mm in height, and 40mm in width. In our experiments, the wood board was placed in front of the robot on the cement pavement where the right and left legs must cross over one after another compliantly.

A. Experimental Results

TABLE I
Limits on Velocities, Accelerations and Jerks of Hip Joint and Knee Joint

Item	Hip	Knee
Limited velocity (deg/s)	10	20
Limited acceleration (deg/s^2)	20	20
Limited jerk (deg/s^3)	40	50

Units in the above table are expressed as: deg = degree, s = second.

First, we program the path trajectories of striding the obstacle. Thirteen waypoints are selected according to the mixed parabola method illustrated in section III. Thirty millimeters of the safety margin is set to avoid the collision of the wood board and the front legs. At the beginning and the end of the crossing behavior the legs are in stance phrase, so the velocities can be set approximately to zeros. The driving devices of all the hip joints are absolutely identical and the ones of the knee joints are the same as well. Thus, the constraints of velocities, accelerations, and jerks at the waypoints given in Table I are appropriate to four legs.

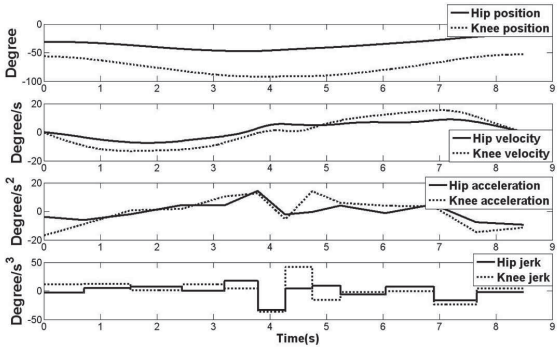

Fig. 6. Optimal trajectories for the RF hip and RF knee joint. The time axes start from zero for convenience.

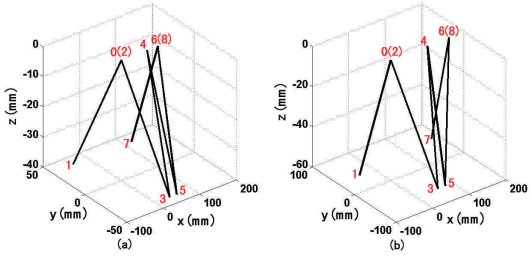

Fig. 7. COG trajectories. (a) is the COG trajectory of a circle for normal periodic motion, and (b) is the COG trajectory for jumping obstacle of the front legs. The numbers from 0 to 8 on the trajectories are the characteristic points indicating the COG travelling direction.

Through optimizing the trajectory generation problem with the accelerated hybrid penalty function method, we get the optimal time interval vector as $\mathbf{h}$ = [0.7135, 0.8235, 0.9064, 0.7554, 0.5917, 0.4912, 0.4739, 0.4993, 0.7962, 0.8531, 0.7611, 0.8329], and the total time is 8.4982s. Taking the RF leg for example, the planned positions, velocities, accelerations, and jerks trajectories of the hip and knee joints can be obtained as shown in Fig. 6.

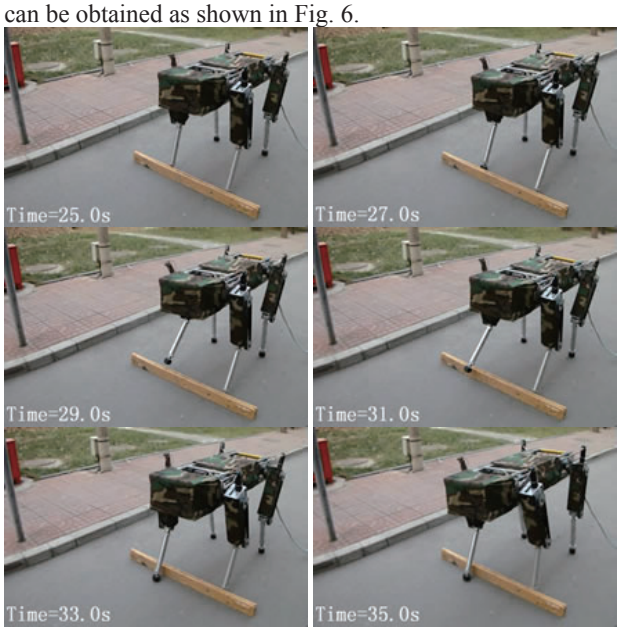

(a)

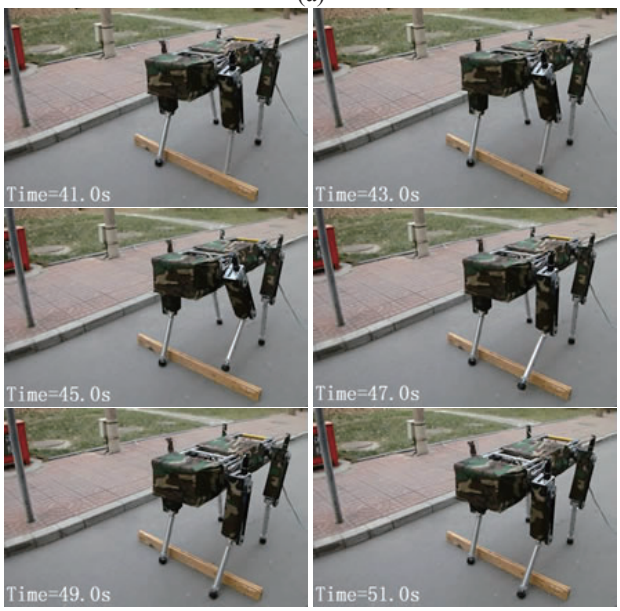

(b)

Fig. 8. Snapshots of the FROG-I robot striding the wood board with front legs, including (a) RF leg from 25.0s to 35.0s and (b) LF leg from 41.0s to 51.0s.

Based on the smooth traversing trajectories and proper COG adjustments shown in Fig. 7, the robot can overstride the obstacle and maintain periodic motion depending on the joint-level precision positioning controller. The videos of

obstacle striding can be downloaded in the topic of trajectory planning at the website of [21]. Fig. 8 demonstrates the snapshots of the front legs striding over the obstacle.

B. Evaluations

As presented in the experimental results, the quadruped robot strides the obstacle flexibly and compliantly on the whole. Some detailed performance of the results is discussed.

From the comparison of COG trajectories of Fig. 7(a) and Fig. 7(b) we can draw the conclusion that to facilitate the striding, the robot increases the travelling distance within a period. Meanwhile, more potential energy is generated to keep the stability with the increment of roll inclination before the time of lifting up legs, which is derived from the extremely stretched or flexed legs. On the contrary, the serious roll inclination weakens the robot's whole compliance. Consequently, in the next work the COG trajectories' smoothness can be enhanced to improve the compliance while producing enough stability margins and potential energy simultaneously.

In Fig. 8, there are some differences between the crossing behaviors of the RF leg and the LF leg. The obvious phenomenon is that after both of the legs' arriving at the ground, the distances from the footholds to the board are not equal strictly. The two reasons for this are the mechanical clearance, which exists in joint junctions and the transmission systems, and the tiny slippage that results from the less friction forces between the feet and the nature ground. So the quadruped robot's behaviors occasionally deviate from the planned scheme slightly.

VI. Conclusions and Future Work

In this paper we have presented an effective control approach for the realization of obstacle striding with compliance. The method uses Rodrigues rotation formula to build the forward kinematics model and the numerical solution is applied into the inverse kinematics problem. To find the rational waypoints for crossing over obstacles, the trajectories are planned with a mixed parabola method. The joint-space optimization with restricted velocities, accelerations, and jerks generates efficient and smooth trajectories that the joints should follow up. We also investigate the strategy of COG trajectories adjustment for periodic motion and striding movement. The COG trajectories make sure that the quadruped robot always in proper posture while walking and obstacle striding. The experiments of the control method is implemented on the FROG-I robot in outdoor environment, and the results demonstrate the high-performance of compliant walking and obstacle striding.

As the problems stated in Section V-B, we plan to create twice differentiable COG trajectories to reduce the vibration while walking. Furthermore, the gyroscope and the camera will be used to realize real-time planning for locomotion on discontinuous terrain.

References

[1] H. Kimura, Y. Fukuoka, and A. H. Cohen, "Adaptive dynamic walking of a quadruped robot on irregular terrain based on biological concepts," *The International Journal of Robotics Research*, vol. 26, no. 5, 2007, pp. 475-490.

[2] H. Kimura, Y. Fukuoka, K. Konaga, Y. Hada, and K. Takase, "Towards 3D adaptive dynamic walking of a quadruped robot on irregular terrain by using neural system model," in *IEEE/RSJ International Conference on Intelligent Robots and Systems*, vol. 4, 2001, pp. 2312-2317.

[3] I. Poulakakis, J. A.. Smith, and M. Buehler, "Modeling and experiments of untethered quadrupedal running with a bounding gaits: the Scout II robot," *The International Journal of Robotics Research*, vol. 24, no. 4, 2005, pp. 239-256.

[4] P. G. de Santos, J. A. Galvez, J. Estremera, and E. Garcia, "SILO4—A true walking robot for the comparative study of walking machine techniques," *IEEE Robotics & Automation Magazine*, vol. 10, no. 4, 2003, pp. 23-32.

[5] J. Estremera, and P. G. de Santos, "Generating continuous free crab gaits for quadruped robot on irregular terrain," *IEEE Transactions on Robotics Research*, vol. 21, no. 6, 2005, pp. 1067-1076.

[6] J. Z. Kolter, M. P. Rodgers, and A. Y. Ng, "A control architecture for quadruped locomotion over rough terrain," in *IEEE International Conference on Robotics and Automation*, 2008, pp. 811-818.

[7] M. Kalakrishnan, J. Buchli, P. Pastor, M. Mistry, and S. Schaal, "Fast, robust quadruped locomotion over challenging terrain," in *IEEE International Conference on Robotics and Automation*, 2010, pp. 2665-2670.

[8] Bin Li, Xun Li, Wei Wang, Yanfeng Tang, and Yiping Yang, "A method based on central pattern generator for quadruped leg control," in *IEEE International Conference on Robotics and Biomimetics*, vol.15, 2009, pp. 2035–2041.

[9] M. Mistry, J. Buchli, and S. Schaal, "Inverse dynamics control of floating base systems using orthogonal decomposition," in *IEEE International Conference on Robotics and Automation*, 2010, pp. 3406-3412.

[10] S. Kajita, H. Hirukawa, K. Yokio, and K. Harada, "Humanoid Robots," Tsinghua University Press, 2008, pp. 17-53.

[11] D. Pongas, M. Mistry, and S. Schaal "A robust quadruped walking gait for traversing rough terrain," in *IEEE International Conference on Robotics and Automation*, 2007, pp. 1474-1479.

[12] A. Hait, T. Simenon, and M. Taix, "Robust motion planning for rough terrain navigation," in *IEEE/RSJ International Conference on Intelligent Robots and Systems*, vol. 1, 1999, pp. 11-16.

[13] X. D. Chen, K. Watanabe, K. Kiguchi, and K. Izumi, "Translational crawl and path tracking of a quadruped robot," *Journal of Robotic Systems*, vol. 9, no. 12, 2002, pp. 569-584.

[14] S. H. Park, and G. J. Chung, "Quasi-static obstacle crossing of an animal type four-legged walking machine," *Journal of Robotica*, vol. 18, no. 5, 2000, pp. 519-533.

[15] J. R. Rebula, P. D. Neuhaus, B. V. Bonnlander, M. J. Johnson, and J. E. Pratt, "A controller for the littledog quadruped walking on rough terrain," in *IEEE International Conference on Robotics and Automation*, 2007, pp. 1467-1473.

[16] B. Cao, G. I. Dodds, and G.W. Irwin, "Constrained time-efficient and smooth cubic spline trajectory generation for industrial robots," in *IEE Proceedings Control Theory & Applications*, vol. 144, 1997, pp. 467-475.

[17] J. Z. Kolter, and A. Y. Ng, "Task-space trajectories via cubic spline optimization," in *IEEE International Conference on Robotics and Automation*, 2009, pp. 1675-1682.

[18] C. H. Chen, and V. Kumar, "Motion planning of walking robots in environments with uncertainty," in *IEEE International Conference on Robotics and Automation*, vol. 4, 1996, pp. 3277-3282.

[19] S. Ma, T. Tomiyama, and H. Wada, "Omnidirectional static walking of a quadruped robot," *IEEE Transactions on Robotics*, vol. 21, no. 2, 2005, pp. 152-161.

[20] M. H. Hung, F. T. Cheng, H, L, Lee, and D. E. Orin, "Increasing the stability margin of multilegged vehicles through body sway," *Journal of the Chinese Institute of Engineers*, vol. 28, no. 1, 2005, pp. 39-54.

[21] http://irdc.ia.ac.cn/robot/.